American Transactions on
Engineering & Applied Sciences

http://TuEngr.com/ATEAS, http://Get.to/Research

Computer Modeling of Internal Pressure Autofrettage Process of a Thick-Walled Cylinder with the Bauschinger Effect

Zhong Hu[a*], and Sudhir Puttagunta[a]

[a] *Department of Mechanical Engineering, South Dakota State University, USA*

ARTICLEINFO

Article history:
Received January 13, 2012
Accepted January 27, 2012
Available online
January, 28 2012

Keywords:
Thick-walled cylinder;
Internal Pressurize;
Autofrettage;
Bauschinger effect;
Finite Element Analysis

ABSTRACT

In this paper, the internally pressure overloading autofrettage process of a thick-walled cylinder has been numerically investigated. The corresponding axi-symmetric and plane-stress finite element model has been employed. The elasto-plastic material model with nonlinear strain-hardening and kinematic hardening (the Bauschinger effect) was adopted. The residual stresses in the thick-walled cylinder induced by internal autofrettage pressure have been investigated and optimized. The optimum autofrettage pressure and the maximum reduction percentage of the von Mises stress in the autofrettaged thick-walled cylinder under the elastic-limit working pressure have been found, the differences of stress and strain distribution between adopting the Bauschinger-effect and the non-Bauschinger-effect have been compared.

1. Introduction

Thick-walled cylinders subjected to high internal pressure and/or elevated temperature are widely used in the nuclear and chemical industries involving pressures as high as 1380 MPa and

*Corresponding author (Z.Hu). Tel/Fax: +1-605-688-4817. E-mail address: Zhong.Hu@sdstate.edu. ©2012. American Transactions on Engineering & Applied Sciences. Volume 1 No.2 ISSN 2229-1652 eISSN 2229-1660. Online Available at http://TUENGR.COM/ATEAS/V01/143-161.pdf

temperatures of up to 300 °C, (Ford et al. 1981) especially for military applications involving transient peak internal pressures as high as 350 MPa and temperature of up to 1500 °C inside the gun barrel in a ballistic event. (Bundy et al. 1996) In the absence of residual stresses, cracks usually form at the bore where the hoop stress developed by the working pressure is highest. (Daniels 1942; Zapfec 1942; Bush 1988; Masu and Graggs 1992) To prevent such failure and to increase the pressure-carrying capacity, a common practice is autofrettage treatment of the cylinder prior to use. Autofrettage is used to introduce advantageous favorable compressive residual hoop stress inside wall of a cylinder and result in an increase in the fatigue lifetime of the component. There are basically three types of autofrettage. These are carried out by hydraulic pressurization, by mechanically pushing an oversized mandrel, or by the pressure of powder gas, (Davidson and Kendall 1970; Malik and Khushnood 2003) in which hydraulic and powder gas pressurization are based on the same principal and strengthening mechanism. In general, vessels under high pressure require a strict analysis for an optimum design for reliable and secure operational performance. Prediction of residual stress field and optimization of the autofrettage processes' parameters are some of the key issues in this context, which normally involve a careful evaluation of the related modeling, simulation and experimental details. (Davidson et al. 1963; Chu and Vasilakis 1973; Shannon 1974; Tan and Lee 1983; Gao 1992; Avitzur 1994; Kandil 1996; Lazzarin and Livieri 1997; Zhu and Yang 1998; Venter et al. 2000; Gao 2003; Iremonger and Kalsi 2003; Kihiu et al. 2003; Parker et al. 2003; Perry and Aboudi 2003; Zhao et al. 2003; Perl and Perry 2006; Bihamta et al. 2007; Hojjati and Hassani 2007; Korsunsky 2007; Gibson 2008; Perry and Perl 2008; Ayob et al. 2009; Darijani et al. 2009) Efforts are continually made in the regarding aspects.

Overloading pressure autofrettage process involves the application of high pressure to the inner surface of a cylinder, until the desired extent of plastic deformation is achieved. Analytical solution of pressure autofrettage of a constant cross-section cylinder, subject to some end conditions, is possible through the use of simplifying assumptions, such as choice of yield criteria and material compressibility and, critically, material stress-strain behavior. On the other hand, autofrettage causes large plastic strains around the inner surface of a cylinder, which noticeably causes the early onset of non-linearity when remove the autofrettage pressure in the unloading process – a kinematic hardening phenomenon termed the Bauschinger effect. This non-linearity typically causes significant deviation from those material models that are often assumed. The effect is most pronounced around the inner surface, and in turn has a significant effect on the residual

stresses developed when the autofrettage load is removed, especially as it can cause reverse yielding to occur when it otherwise would not be expected. Research has been done on this issue with theoretical analysis mostly based on bilinear kinematic hardening (linear elastic and linear hardening) material model which is a good approximation for small strain. (Lazzarin and Livieri 1997; Venter et al. 2000; Kihiu et al. 2003; Parker et al. 2003; Perry and Aboudi 2003; Huang 2005; Perl and Perry 2006; Korsunsky 2007). However, the practical material model is of nonlinear kinematic hardening and with equivalent strain up to 0.5~1% in the autofrettage process, which gives complexity to theoretical analysis using nonlinear kinematic hardening material model. In this paper, the internally pressure overloading autofrettage process will be numerically investigated. An axi-symmetric and plane stress (for open-ended cylinder) finite element model will be presented. The elasto-plastic nonlinear material constitutive relationship will be adopted, incorporating a nonlinear kinematic hardening (the Bauschinger effect) for which no analytical solution exists. The effects of the autofrettage pressure on the residual stresses in a thick-walled cylinder will be evaluated. The percentage of stress reduction by autofrettage treatment will be calculated based on von Mises yield criterion. The optimum autofrettage pressure will be found. The differences of stress and strain distribution between adopting the Bauschinger-effect and the non-Bauschinger-effect will be compared.

2. Mathematical Model

In this work, the thick-walled cylinder is made of stainless steel AISI 304. An elasto-plastic governing equations for material behavior with a homogeneous and isotropic hardening model is used. The true stress – true strain behavior of the strain hardening material follows the Hooke's law in the elastic region, and, for comparison purpose, the power-law hardening in the plastic region, (Hojjati and Hassani 2007)

$$\sigma = \begin{cases} E\epsilon & \epsilon < \epsilon_y \\ K\epsilon^n & \epsilon \geq \epsilon_y \end{cases} \quad (1),$$

where σ and ϵ are true stress and true strain, respectively. ϵ_y is the strain at the yield point. E is the modulus of elasticity. K is a material constant equal to $K = \sigma_y \epsilon_y^{-n} = \sigma_y^{1-n} E^n$, and n is the strain-hardening exponent of the material ($0 \leq n < 1$). σ_y is the yield stress. Table 1 lists the basic

*Corresponding author (Z.Hu). Tel/Fax: +1-605-688-4817. E-mail address: Zhong.Hu@sdstate.edu. Volume 1 No.2 ISSN 2229-1652 eISSN 2229-1660. Online Available at http://TUENGR.COM/ATEAS/V01/143-161.pdf

parameters and material data and derived material parameters to be used in the FEA modeling. (Peckner and Bernstein 1977; Harvey 1982; Boyer et al. 1985; ASM International Handbook Committee 1990). Figure 1 shows the elasto-plastic stress-strain relationship with kinematic hardening (the Bauschinger effect). Commercially available software ANSYS has been used for finite element modeling of the autofrettaged thick-walled cylinder. (Swanson Analysis System Inc. 2011) The finite element model is shown in Figure 2. The element PLANE183 with the capacity of elastic and plastic material nonlinearity and non-linear kinematic hardening (the Bauschinger-effect) has been adopted, which is an eight-node plane-stress 2-D element with higher accuracy quadratic shape function. In order to get reasonable accuracy, more elements are used near inner surface and outer surface of the cylinder, see Figure 2.

Table 1: Model dimensions and material properties.

Material of the Cylinder	AISI304
Modulus of Elasticity E	196.0 GPa
Poisson's Ratio υ	0.29
Yield Strength σ_y	152.0 MPa*
Strain at Yield Point ϵ_y	7.755×10^{-4}
Strain-Hardening Exponent n	0.2510
Material Constant K	917.4 MPa
Inner Radius a	60 mm
Outer Radius b	90 mm
Maximum Working Pressure p_i	47.22MPa

* corresponding to 215MPa at 0.2% offset and ultimate tensile strength of 505 MPa.

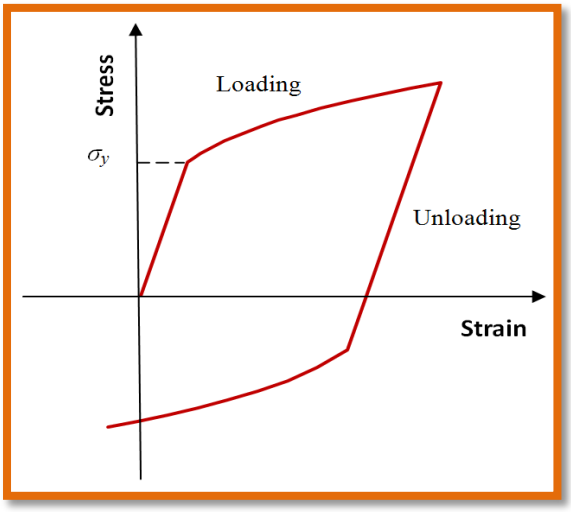

Figure 1: The elasto-plastic stress – strain model with kinematic hardening (the Bauschinger effect).

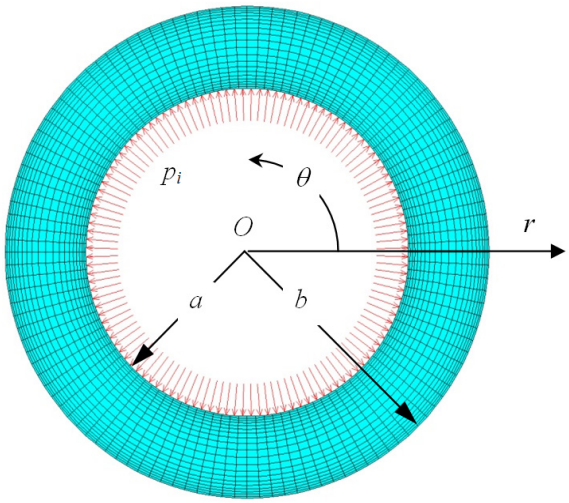

Figure 2: Finite element model of a plane-stress thick-walled cylinder.

3. Modeling Results and Discussions

Consider a thick-walled cylinder having inner radius a and outer radius b and subjected to the internal pressure p_i as shown in Figure 2. The material will obey the Hooke's law when it is within the elastic region. This allow us to use the Lame's equations for calculating the hoop stress, σ_θ, and radial stress, σ_r, along the thickness of the cylinder, when the ends of the cylinder are open and unconstrained so that the cylinder is in a condition of plane stress. (Ugural 2008)

$$\sigma_\theta = \frac{a^2 p_i}{b^2 - a^2}\left[1 + \left(\frac{b^2}{r^2}\right)\right] \quad (2),$$

$$\sigma_r = \frac{a^2 p_i}{b^2 - a^2}\left[1 - \left(\frac{b^2}{r^2}\right)\right] \quad (3),$$

$$\sigma_z = 0 \quad (4),$$

Therefore, the von Mises (equivalent) stress is

$$\sigma_i = \left(\sigma_\theta^2 + \sigma_r^2 - \sigma_\theta \sigma_r\right)^{\frac{1}{2}} = \frac{a^2 p_i}{b^2 - a^2}\left[1 + 3\left(\frac{b}{r}\right)^4\right]^{\frac{1}{2}} \quad (5),$$

The radial displacement is

*Corresponding author (Z.Hu). Tel/Fax: +1-605-688-4817. E-mail address: Zhong.Hu@sdstate.edu. Volume 1 No.2 ISSN 2229-1652 eISSN 2229-1660. Online Available at http://TUENGR.COM/ATEAS/V01/143-161.pdf

$$u = \frac{a^2 p_i r}{E(b^2 - a^2)}\left[(1-\nu) + (1+\nu)\frac{b^2}{r^2}\right] \quad (6),$$

Obviously, the maximum von Mises stress is at $r = a$. Assuming von Mises yield criterion applied, i.e., $\sigma_i \leq \sigma_y$, so by substituting the data from Table 1, the maximum applied working pressure (the maximum internal pressure without causing yielding) is

$$p_{w_{max}} = \sigma_y \frac{b^2 - a^2}{a^2}\left[1 + 3\left(\frac{b}{a}\right)^4\right]^{-\frac{1}{2}} = 47.2 \text{ (MPa)} \quad (7),$$

Figure 3 shows the analytical and modeling results of stress components and radial displacement along the thickness of the cylinder subjected to the maximum working pressure ($p_{w\ max}$ = 47.2 MPa). The modeling results are well agreed with the analytical results from Lame's equations, indicating the reliability of the model employed in the numerical analysis. Figure 3 also shows that the maximum von Mises stress and hoop stress located at the inner surface of the cylinder, and the hoop stress is the major stress component causing yield failure.

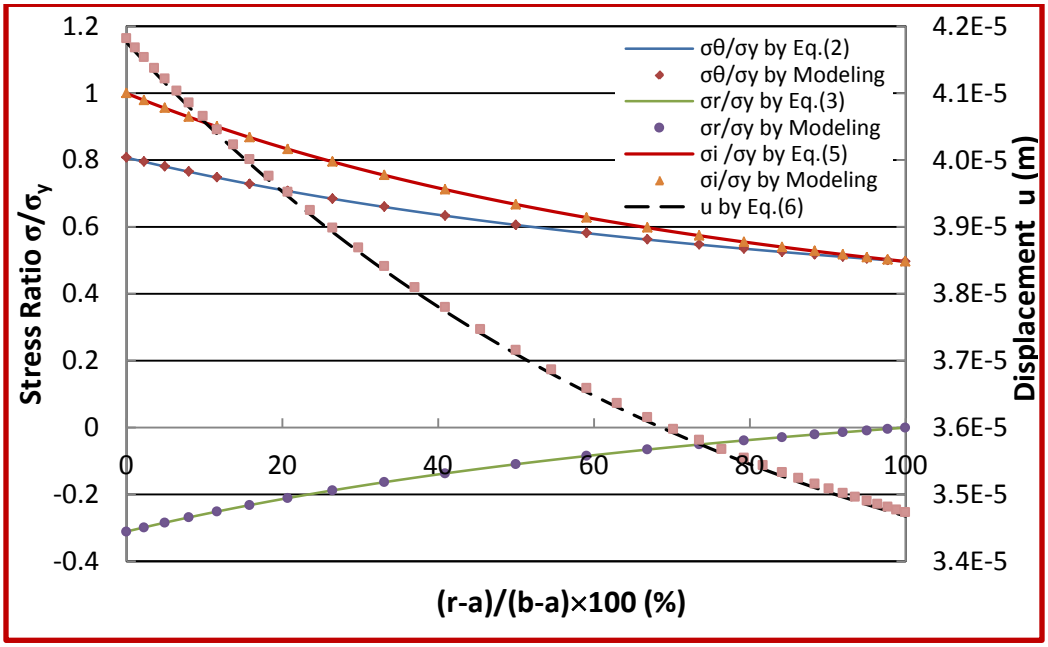

Figure 3: Analytical and modeling results of stresses and radial displacement along the thickness of the cylinder subjected to the maximum working pressure ($p_{w\ max}$ = 47.2 MPa).

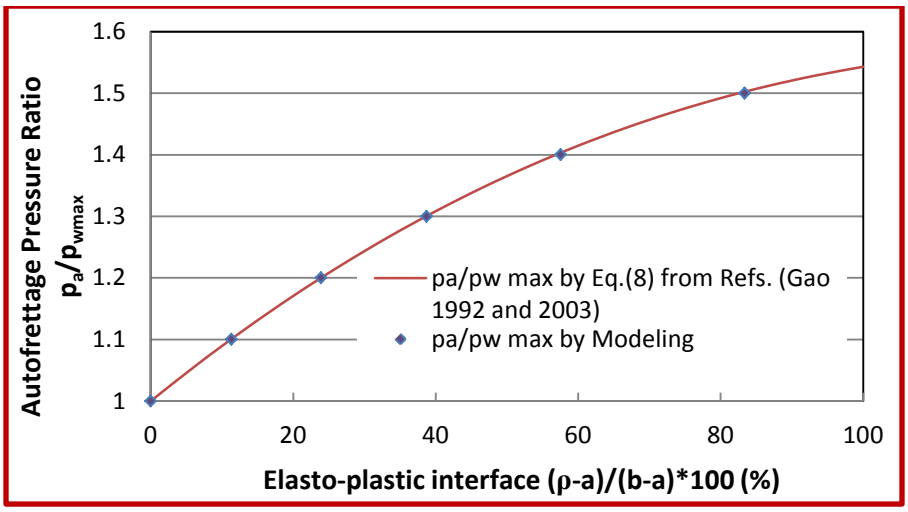

Figure 4: The relationship of elastic-plastic interface ρ and the autofrettage pressure p_a.

As the internal pressure increasing, yielding (plastic deformation) starts from cylinder's inner surface and gradually extends towards cylinder's outer surface. This process is basically an elastic-plastic deformation process. The relation between internal autofrettage pressure, p_a, and the radius of the elastic-plastic boundary (interface) in plane stress condition, ρ, is determined by (Gao 1992; Gao 2003)

$$\begin{cases} \frac{p_a}{\sigma_y} = \frac{2}{\sqrt{3}}\left[\frac{\cos(\varphi_\rho+\varphi_n)}{\cos(\varphi_a+\varphi_n)}\right]^{\frac{(3n^2+n)}{(3n^2+1)}} exp\left[\frac{\sqrt{3}n(n-1)}{3n^2+1}(\varphi_a-\varphi_\rho)\right]\cos\varphi_a, \\ \rho = a\sqrt{\frac{\sin(\varphi_a+\pi/6)}{\sin(\varphi_\rho+\pi/6)}}\left[\frac{\cos(\varphi_\rho+\varphi_n)}{\cos(\varphi_a+\varphi_n)}\right]^{\frac{2n}{(3n^2+1)}} exp\left[\frac{\sqrt{3}}{2}\frac{1-n^2}{3n^2+1}(\varphi_\rho-\varphi_a)\right], \\ \varphi_\rho = \cos^{-1}\left[\frac{\sqrt{3}}{2}\frac{(b^2-\rho^2)}{\sqrt{3b^4+\rho^4}}\right], \end{cases} \quad (8),$$

Where

$$\varphi_n = \cos^{-1}\left(\frac{\sqrt{3n}}{\sqrt{3n^2+1}}\right) \quad (9),$$

During autofrettage process, the elastic-limit pressure p_e (pressure at which yielding commences at inner surface) is obviously $\frac{p_e}{p_{w\,max}} = 1$ and $\rho = a$ in the given case, and the plastic-limit pressure p_y (pressure at which plasticity has spread throughout the cylinder) is

*Corresponding author (Z.Hu). Tel/Fax: +1-605-688-4817. E-mail address: Zhong.Hu@sdstate.edu. Volume 1 No.2 ISSN 2229-1652 eISSN 2229-1660. Online Available at http://TUENGR.COM/ATEAS/V01/143-161.pdf

$\frac{p_y}{p_{w\,max}} = 1.543$ and $\rho = b$ in the given case. Figure 4 shows the relation of elastic-plastic interface ρ and the autofrettage pressure p_a obtained by modeling and analytical approaches, they are well agreed.

Figures 5-7 show the autofrettage stress distributions for the thick-walled cylinder subjected to different internal autofrettage pressure range of $\frac{p_a}{p_{w\,max}} = 1\sim1.6$ by modeling. Hoop stress and von Mises stress in Figures 5 and 7 clearly indicate that by increasing applied autofrettage pressure, elastic-plastic interface (the turning point of the curve corresponding to the position ρ in Figure 4) moves towards the outer surface of the cylinder and eventually reaches the outer surface, while radial stress in Figure 6 indicate that the radial stress in compression, with highest compressive stress in the inner surface and zero in the outer surface, increasing as the autofrettage pressure increasing.

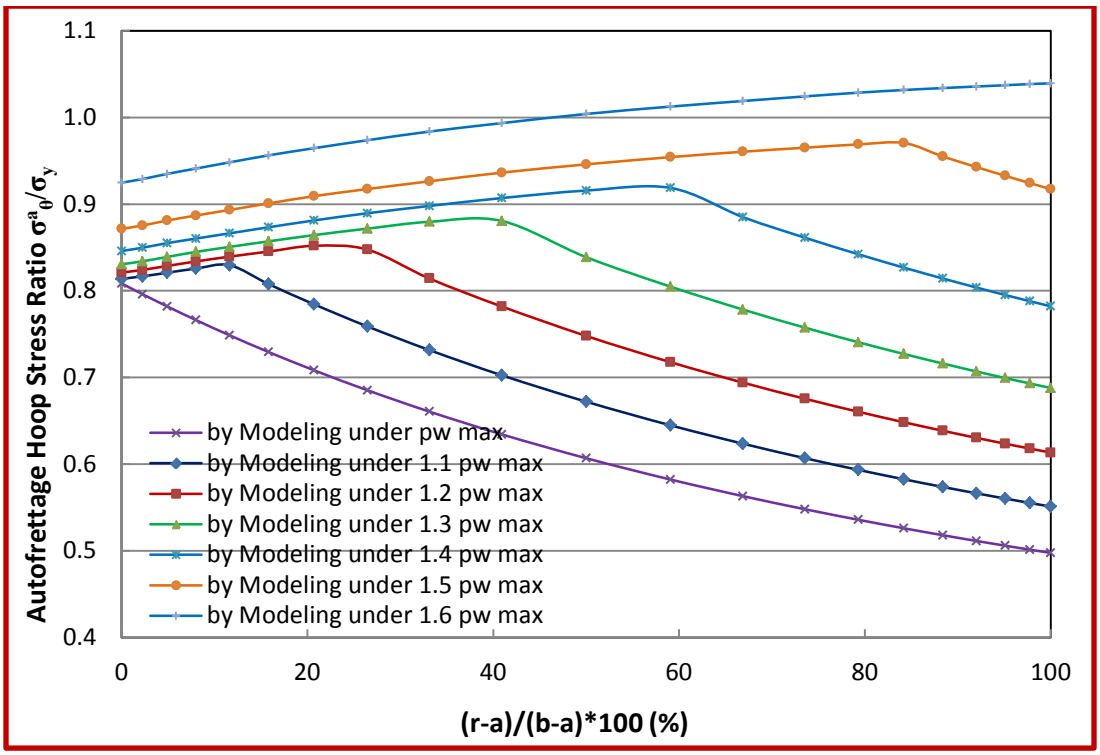

Figure 5: Autofrettage hoop stress distribution under different autofrettage pressure.

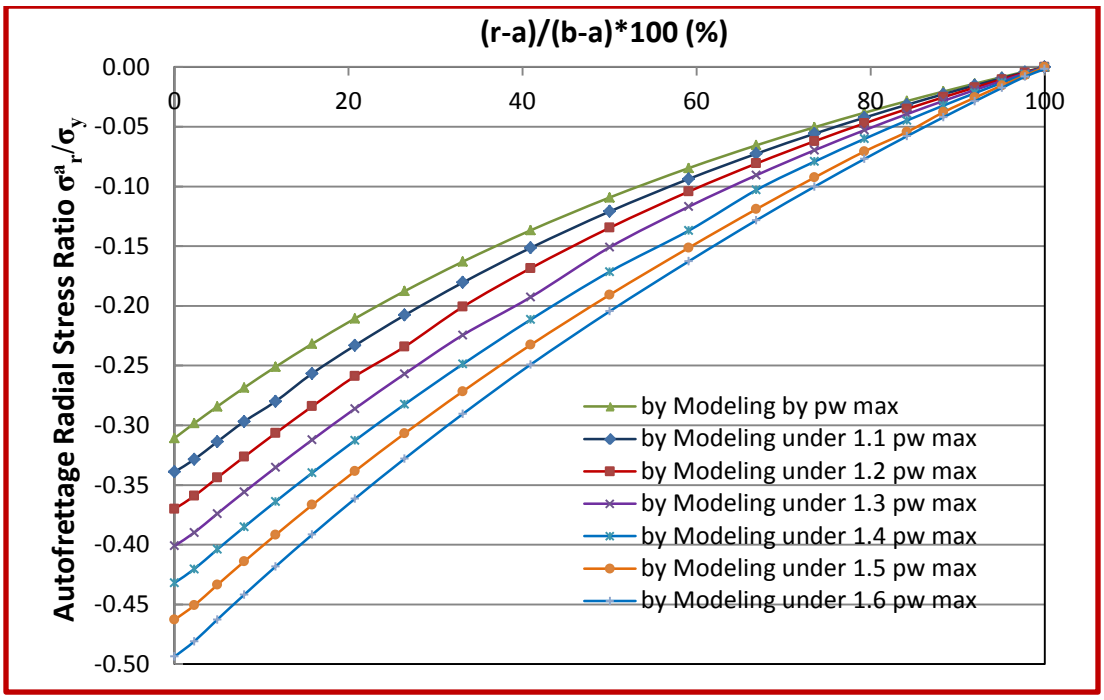

Figure 6: Autofrettage radial stress distribution under different autofrettage pressure.

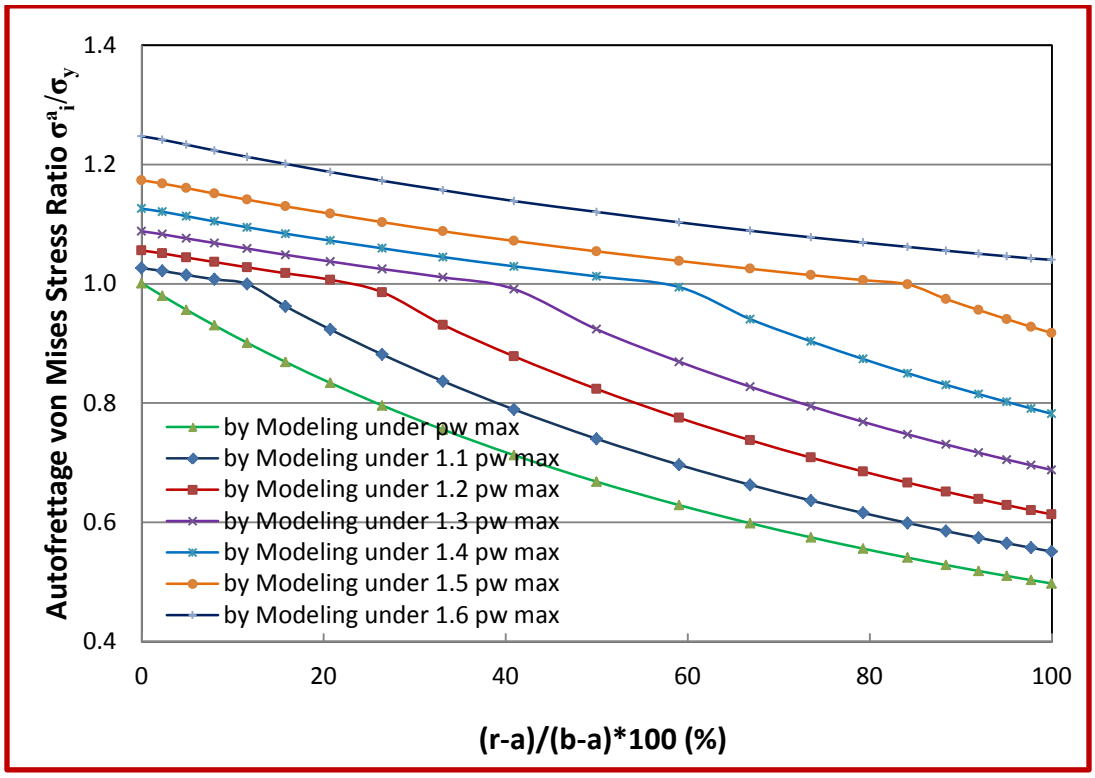

Figure 7: Autofrettage von Mises stress distribution under different autofrettage pressure.

*Corresponding author (Z.Hu). Tel/Fax: +1-605-688-4817. E-mail address: Zhong.Hu@sdstate.edu. American Transactions on Engineering & Applied Sciences. Volume 1 No.2 ISSN 2229-1652 eISSN 2229-1660. Online Available at http://TUENGR.COM/ATEAS/V01/143-161.pdf

When the internal autofrettage pressure is removed, the elastic deformation is trying to resume its original shape while the plastic deformation is resisting this process so that residual stresses within the cylinder have been induced, and the so-called pressure autofrettage process has been accomplished. This unloading process basically is treated elastically. However, reverse yielding is possible if earlier onset happens due to the Bauschinger effect. Figures 8-10 show the residual stress distribution after removed autofrettage pressure. From Figure 8, it shows a compressive residual hoop stress near the inner surface generated which is favorable to the thick-walled cylinder when it is under internal working pressure (partially cancelling the tensile hoop stress induced by the working pressure), and a tensile residual hoop stress near the outer surface of the cylinder. Figure 9 shows a relative smaller but compressive residual radial stress left inside of the thick-wall, satisfying the boundary conditions of zero radial stress on inner surface and outer surface of the cylinder. Figure 10 shows the residual von Mises stress with higher values basically near the inner surface and outer surface of the cylinder. The turning points of the curves in Figures 8 and 10 are almost the same as in Figures 5 and 7 indicates that the earlier onset of the reverse yielding is very less, not changing the elastic-plastic interface very much.

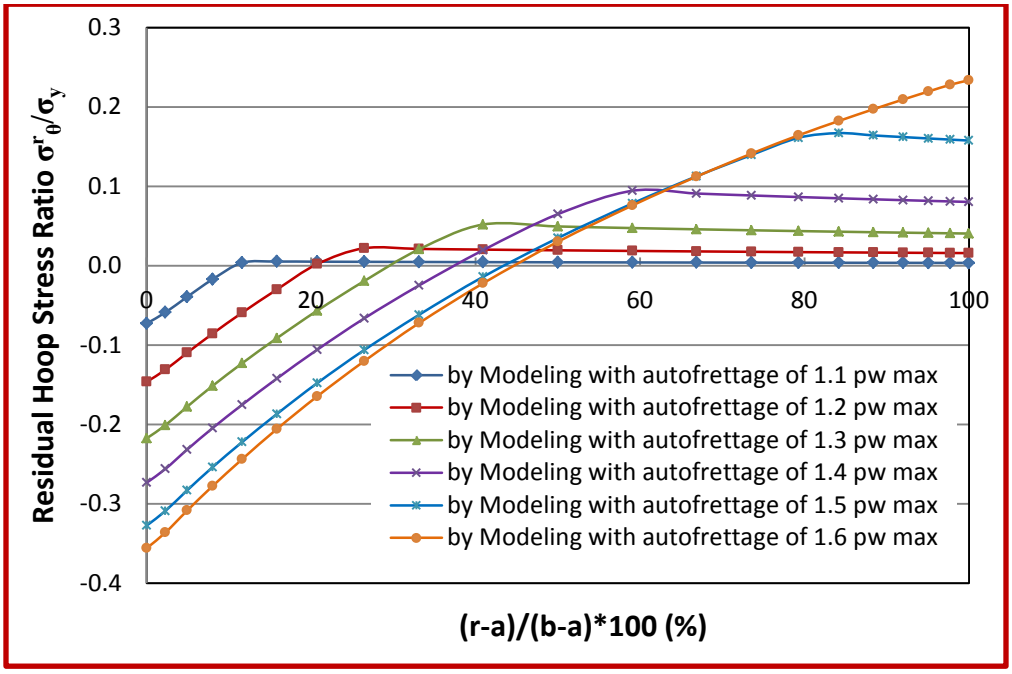

Figure 8: Residual hoop stress distribution after removed the autofrettage pressure.

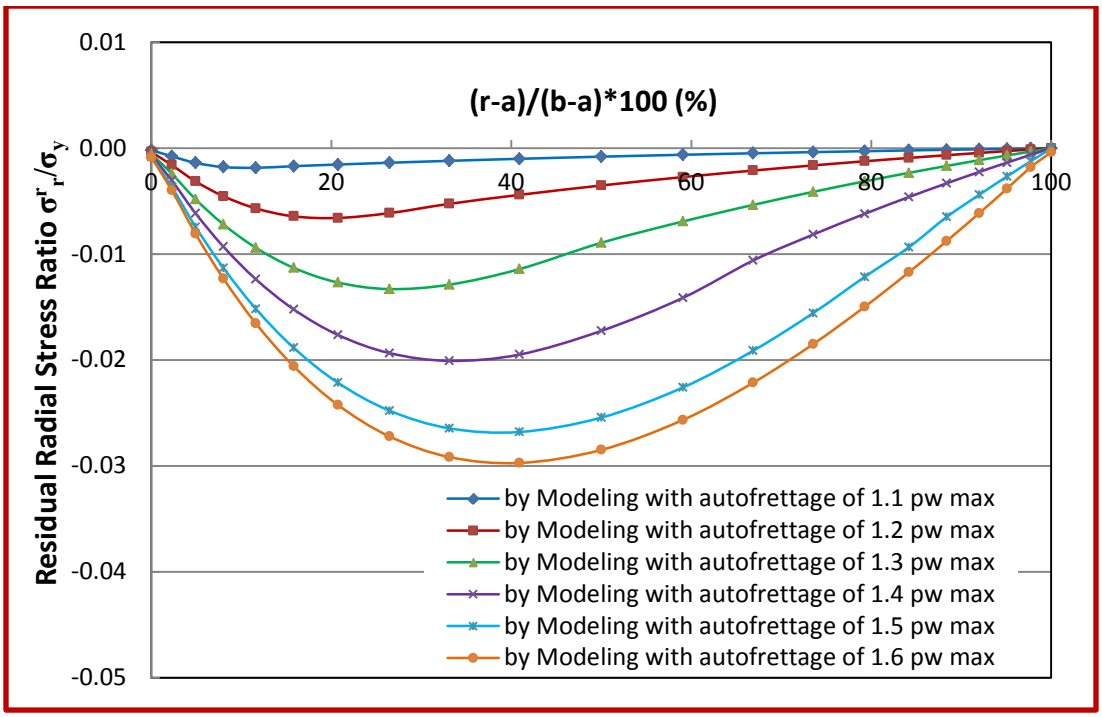

Figure 9: Residual radial stress distribution after removed the autofrettage pressure.

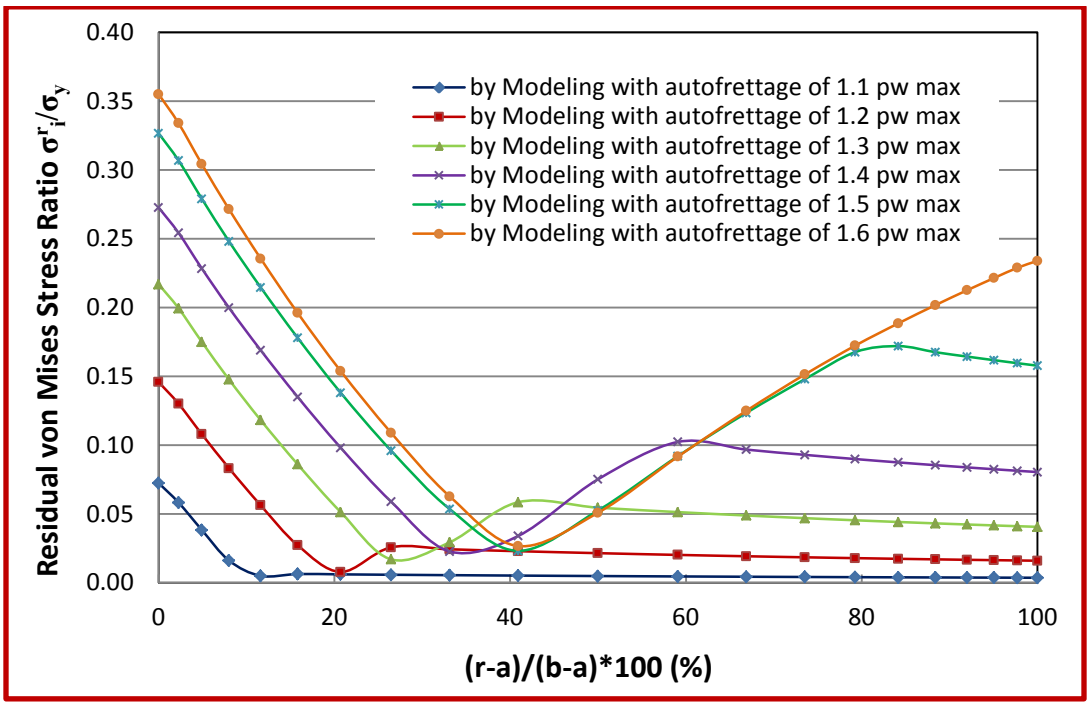

Figure 10: Residual von Mises stress distribution after removed the autofrettage pressure.

*Corresponding author (Z.Hu). Tel/Fax: +1-605-688-4817. E-mail address: Zhong.Hu@sdstate.edu. Volume 1 No.2 ISSN 2229-1652 eISSN 2229-1660. Online Available at http://TUENGR.COM/ATEAS/V01/143-161.pdf

When an autofrettaged thick-walled cylinder is applied to an internal working pressure, this reloading process is treated elastically, since a plastic deformation is not desired in the application of the cylinders based on the static yield design criterion. Figures 11-13 show the stress distributions of an autofrettaged thick-walled cylinder after reloading by an elastic-limit pressure (i.e., the maximum working pressure $p_{w\,max} = 47.2$ MPa). It shows more uniform distribution of the stress components and von Mises stress throughout the thickness of the cylinder due to the autofrettage treatment, which makes maximum von Mises stress in the cylinder less than that without autofrettage treatment. However, radial stress has not been changed very much, see Figure 12. Figure 14 shows the relationship of the final maximum von Mises stress versus autofrettage pressure for a thick-walled cylinder under the maximum working pressure ($p_{w\,max}$ = 47.2 MPa). It clearly shows the optimal autofrettage pressure is about 1.5 times the maximum working pressure, and the maximum von Mises stress reduction with this autofrettage pressure is about 28%.

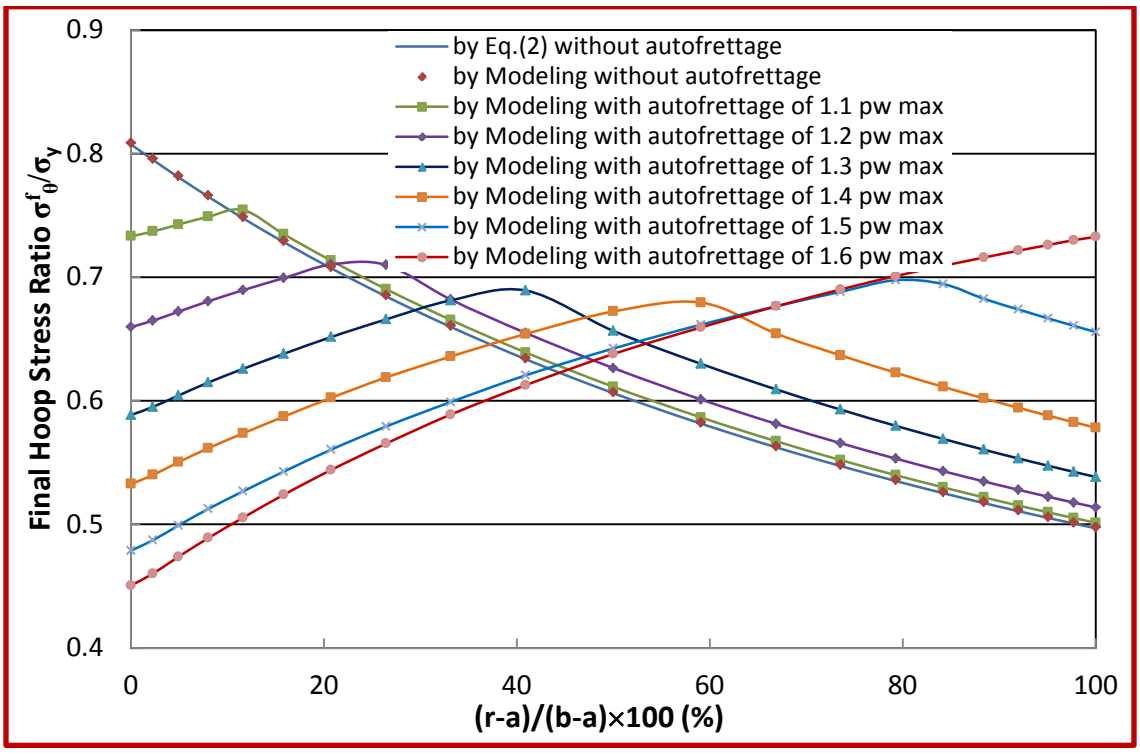

Figure 11: Final hoop stress distribution of an autofrettaged thick-walled cylinder under the maximum working pressure ($p_{w\,max}$ = 47.2 MPa).

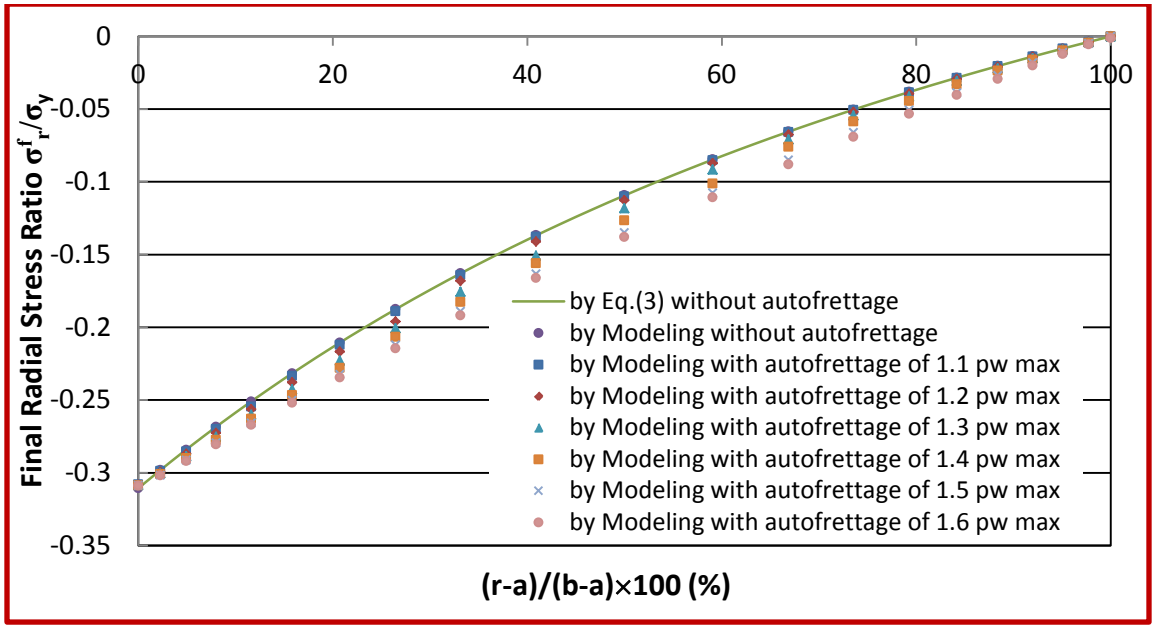

Figure 12: Final radial stress distribution of an autofrettaged thick-walled cylinder under the maximum working pressure ($p_{w\ max}$ = 47.2 MPa).

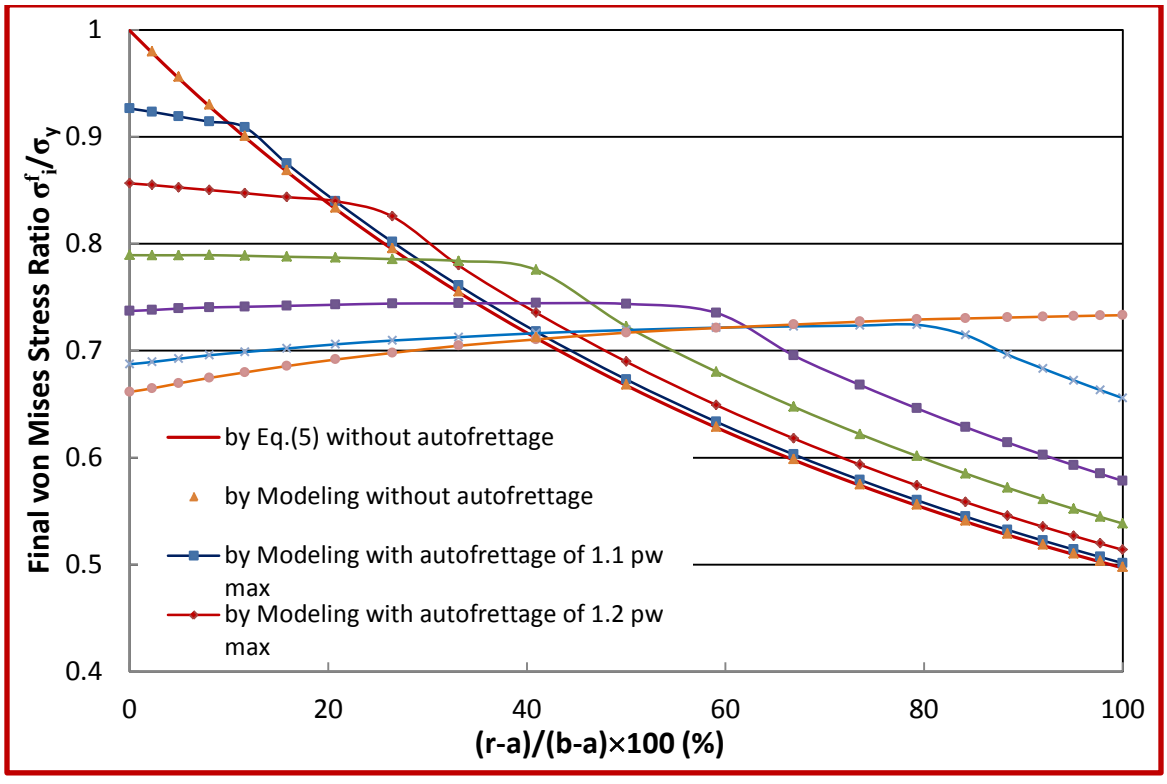

Figure 13: Final von Mises stress distribution of an autofrettaged thick-walled cylinder under the maximum working pressure ($p_{w\ max}$ = 47.2 MPa).

*Corresponding author (Z.Hu). Tel/Fax: +1-605-688-4817. E-mail address: Zhong.Hu@sdstate.edu. Volume 1 No.2 ISSN 2229-1652 eISSN 2229-1660. Online Available at http://TUENGR.COM/ATEAS/V01/143-161.pdf

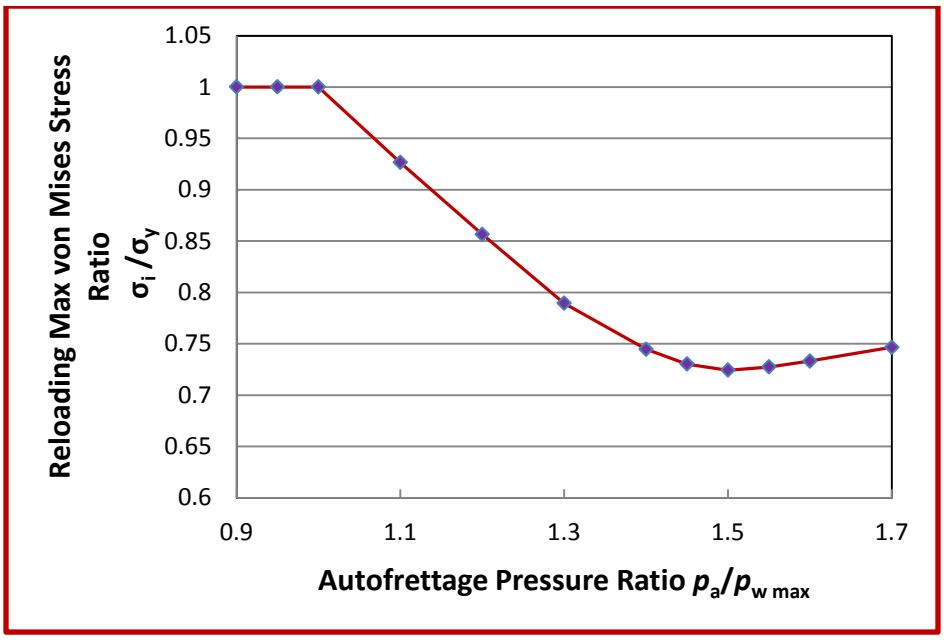

Figure 14: Final maximum von Mises stress versus autofrettage pressure for a thick-walled cylinder under the maximum working pressure ($p_{w\ max}$ = 47.2 MPa).

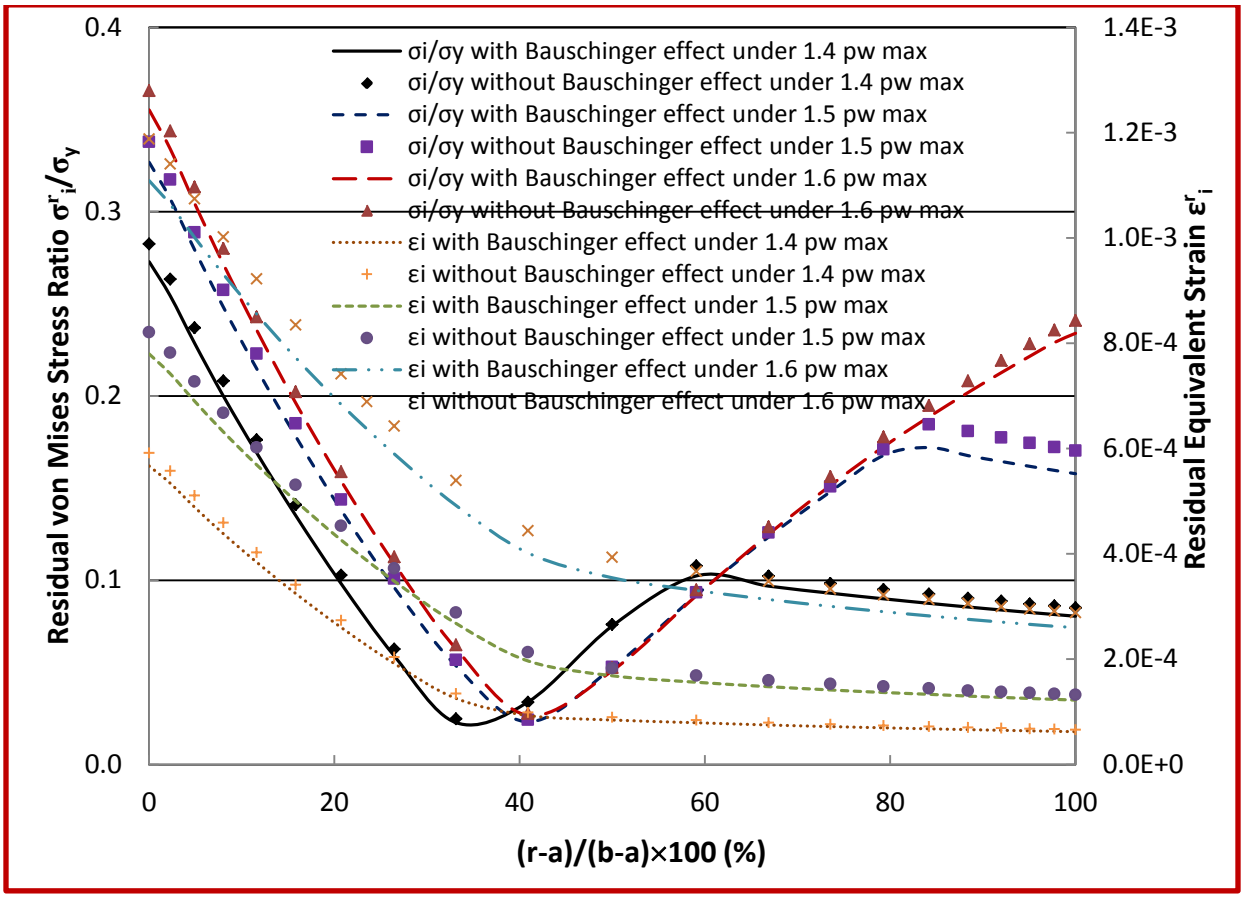

Figure 15: Comparison of residual von Mises stress and equivalent strain with and without the Bauschinger effect.

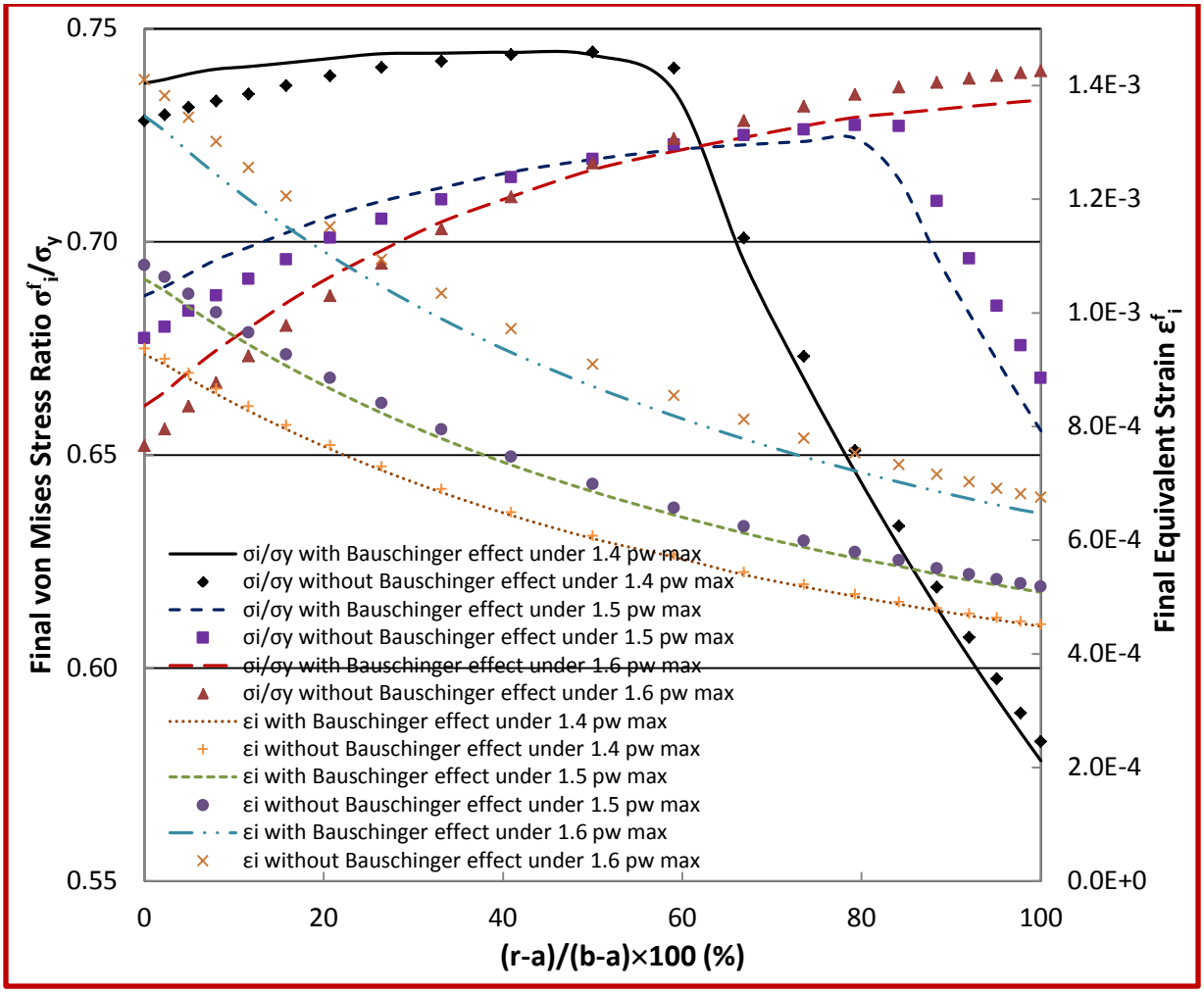

Figure 16: Comparison of final von Mises stress and equivalent strain with and without the Bauschinger effect.

Figure 15 shows the difference of the residual von Mises stress and residual equivalent strain with or without the Bauschinger effect by modeling. It shows a difference between the results by considering the Bauschinger effect or not considering the Bauschinger effect, and an earlier onset of the reverse yielding occurred by modeling with the Bauschinger effect (an earlier turning point) than that without the Bauschinger effect, especially when larger autofrettage pressure applied.

Figure 16 shows the difference of the final von Mises stress and final equivalent strain with or without the Bauschinger effect by modeling. It shows a clear difference between the results by considering the Bauschinger effect or not considering the Bauschinger effect, and a earlier turning

*Corresponding author (Z.Hu). Tel/Fax: +1-605-688-4817. E-mail address: Zhong.Hu@sdstate.edu. Volume 1 No.2 ISSN 2229-1652 eISSN 2229-1660. Online Available at http://TUENGR.COM/ATEAS/V01/143-161.pdf

point by modeling with the Bauschinger effect than that without the Bauschinger effect, especially when larger autofrettage pressure applied, due to the previous generated elastic-plastic interface during the autofrettage process. This phenomenon indicates an earlier yield may occur for an internally pressure autofrettaged thick-walled cylinder under a working pressure by considering the Bauschinger effect. Therefore, in a design of safety, the Bauschinger effect should not be ignored.

4. Conclusions

The Internal pressure overloading autofrettage processes of a thick-walled cylinder have been numerically investigated by finite element analysis, taking into account the elasto-plastic strain hardening material with kinematic hardening (the Bauschinger effect) and the von Mises yield criterion. The corresponding axi-symmetric and plane-stress model has been employed. The residual stresses in the thick-walled cylinder induced by autofrettage pressure have been numerically analyzed and optimized. Under the giving geometric and material condition, the optimum autofrettage pressure has been found to be about 1.5 times the elastic-limit working pressure, and the maximum reduction percentage of the maximum von Mises stress in the autofrettaged thick-walled cylinder under the elastic-limit working pressure has been found to be about 28%. The Bauschinger effect does induce an earlier onset of the reverse yielding for an internally pressure autofrettaged thick-walled cylinder under a working pressure. Therefore, in a design of safety, the Bauschinger effect should not be ignored.

5. Acknowledgements

This work was supported by the State of South Dakota and Mechanical Engineering Department at South Dakota State University, and inspired by the Department of Defense project (Cooperative Agreement # W15QKN-09-2-0002) by METLAB at South Dakota State University.

6. References

ASM International Handbook Committee. (1990). Metals Handbook, 10th ed., vol. 1, , ASM International, Materials Park, OH.

Avitzur, B. (1994). Autofrettage – stress distribution under load and retained stresses after depressurization. *Int. J. Pres. Ves. & Piping*, 57, 271-287.

Ayob, A. B., M. N. Tamin, andM. K. Elbasheer. (2009). Pressure limits of thick-walled cylinders. *Proceedings of the International MultiConference of Engineers and Computer Scientists IMECS2009*, Vol II, 1649-1654, March 18-20, 2009, Hong Kong.

Bihamta, R., M. R. Movahhedy, and A. R. Mashreghi. (2007). A numerical study of swage autofrettage of thick-walled tubes. *Materials & Design*, 28(3), 804-815.

Boyer, H. E., L. Timothy, and T. L Gall. (Eds.) (1985). Metals Handbook, American Society for Metals, Materials Park, OH.

Bundy, M. L., P. J. Conroy, and J. L. Kennedy. (1996). Simulation & experimental in-wall temperature for 120 mm Ammunition. *Defense Science Journal*, 46(4), 223-232.

Bush, S. H. (1988). Statistics of pressure vessels and piping failures. *Journal of Pressure vessel Technology*, 110, 225-233.

Chu, S. C. and J. D. Vasilakis. (1973). Inelastic behavior of thick-walled cylinders subjected to nonproportionate loading. *Experimental Mechanics*, 113-119.

Daniels, F. H. (1942). An interesting boiler explosion. *Transactions of ASME*, 66(2), 81-126.

Darijani, H., M. H. Kargarnovin, and R. Naghdabadi. (2009). Design of thick-walled cylindrical vessels under internal pressure based on elasto-plastic approach. *Materials & Design,* 30(9), 3537-3544.

Davidson, T. E., D. P. Kendall, and A. N. Reiner. (1963). Residual stresses in thick-walled cylinders resulting from mechanically induced overstrain. *Experimental Mechanics*, 3(11), 253-262.

Davidson, T. E., and D. P. Kendall. (1970). The design of pressure vessels for very high pressure operation, *Mechanical Behavior of Materials Under Pressure*, (Pugh H L P, Ed.) Elsevier Co.

Ford, H., E. H. Watson, and B. Crossland. (1981). Thoughts on a code of practice for forged high pressure vessels of monobloc design. *Journal of Pressure Vessel Technology, Transactions of ASME*, 103, 2-8.

Gao, X-L. (1992). An exact elasto-plastic solution for an open-ended thick-walled cylinder of a strain-hardening material. *Int. J. Pres. Ves. & Piping,* 52, 129-144.

Gao, X-L. (2003). Elasto-plastic analysis of an internally pressurized thick-walled cylinder using a strain gradient plasticity theory. *International Journal of Solids and Structures*, 40, 6445-6455.

Gibson, M. C. (2008). Determination of residual stress distributions in autofrettaged thick-walled cylinders. Ph.D. Thesis. Granfield University April 2008.

*Corresponding author (**Z.Hu**). Tel/Fax: +1-605-688-4817. E-mail address: Zhong.Hu@sdstate.edu. Volume 1 No.2 ISSN 2229-1652 eISSN 2229-1660. Online Available at http://TUENGR.COM/ATEAS/V01/143-161.pdf

Harvey, P. D. (editor) (1982). Engineering Properties of Steels. *American Society for Metals*, Metals Park, OH.

Hojjati, M. H., and A. Hassani. (2007). Theoretical and finite-element modeling of autofrettage process in strain-hardening thick-walled cylinders. *Int. J. Pres. Ves. & Piping*, 84, 310-319.

Huang, X. P. (2005). A general autofrettage model of a thick-walled cylinder based on tensile-compressive stress-strain curve of a material. *The Journal of Strain Analysis for Engineering Design*, 40, 599-607.

Iremonger, M. J. and G. S. Kalsi. (2003). A numerical study of swage autofrettage. *J. Pressure Vessel Technol*, 125(3), 347-351.

Kandil, A. (1996). Analysis of thick-walled cylindrical pressure vessels under the effect of cyclic internal pressure and cyclic temperature. *Int. J. Mech. Sci.*, 38(12), 1319-1332.

Kihiu, J. M., S. M. Mutuli, and G. O. Rading. (2003). Stress characterization of autofrettaged thick-walled cylinders. *International Journal of Mechanical Engineering Education*, 31(4), 370-389.

Korsunsky, A. M. (2007). Residual elastic strains in autofrettaged tubes: elastic-ideally plastic model analysis. *Journal of Engineering Materials and Technology,* 129, 77-81.

Lazzarin, P. and P. Livieri. (1997). Different solutions for stress and stress fields in autofrettaged thick-walled cylinders. *Int. J. Pres. Ves. & Piping*, 71, 231-238.

Malik, M. A., and S. Khushnood. (2003). A review of swage – autofrettage process. *11th International Conference on Nuclear Engineering*, ICONE-11-36257 Tokyo, Japan, April 20-23, 2003, 12pages.

Masu, L. M., and G. Craggs. (1992). Fatigue strength of thick walled cylinders containing cross bores with blending features. *Journal of Mech. Eng. Sci.*, 206, 299–309.

Parker, A. P., G. P. O'Hara, and J. H. Underwood. (2003). Hydraulic versus swage autofrettage and implications of the Bauschinger effect. *Journal of Pressure Vessel Technology*, 125, 309-314.

Peckner, D. and I. M. Bernstein. (1977). Handbook of Stainless Steels. McGraw-Hill Book Company, New York, NY.

Perl, M. and J. Perry. (2006). An experimental-numerical determination of the three-dimensional autofrettage residual stress field incorporating Bauschinger effects. *Journal of Pressure Vessel Technology*, 128, 173-178.

Perry, J. and J. Aboudi. (2003). Elasto-plastic stresses in thick walled cylinders. *Transactions of the ASME*, 125, 248-252.

Perry, J. and M. Perl. (2008). A 3-D model for evaluating the residual stress field due to swage

autofrettage. Journal of Pressure Vessel Technology, *Transactions of the ASME,* 130, 041211-1-6.

Shannon, R. W. E. (1974). Stress intensity factors for thick-walled cylinders. *Int. J. Pres. Ves. & Piping*, 2, 19-29.

Swanson Analysis System Inc. (2011). ANSYS 13.0 User's Manual, Houston.

Tan, C. L. and K. H. Lee. (1983). Elastic-plastic stress analysis of a cracked thick-walled cylinder. *Journal of Strain Analysis*, 18(4), 253-260.

Ugural, A. C. (2008). Mechanics of Materials, John Wiley & Sons. Inc, NJ.

Venter, A. M., R. R. de Swardt, and S. Kyriacon. (2000). Comparative measurements on autofrettaged cylinders with large Bauschinger reverse yield zones. *Journal of Strain Analysis,* 35(6), 459-469.

Zapfec, C. A. (1942). Boiler embrittlement. *Transactions of ASME*, 66(2), 81–126.

Zhao, W., R. Reshadri, and R. N. Dubey. (2003). On thick-walled cylinder under internal pressure. *Journal of Pressure Vessel Technology,* 125, 267-273.

Zhu, R. and J. Yang. (1998). Autofrettage of thick cylinders, *Int. J. Pres. Ves. & Piping*, 75, 443-446.

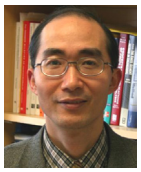

Dr. Zhong Hu is an Associate Professor of Mechanical Engineering at South Dakota State University. He received his BS and Ph.D. in Mechanical Engineering from Tsinghua University. He has worked for railway manufacturing industry as a senior engineer, Tsinghua University as a professor, Japan National Laboratory as a fellow, Cornell University, Penn State University and Southern Methodist University as a research associate. He has authored about 70 publications in the journals and conferences in the areas of nanotechnology and nanoscale modeling by quantum mechanical/molecular dynamics (QM/MD); development of renewable energy related materials; mechanical strength evaluation and failure prediction by finite element analysis (FEA) and nondestructive engineering (NDE); design and optimization of advanced materials (such as biomaterials, carbon nanotube, polymer and composites).

Sudhir Puttagunta is a graduate student in the Department of Mechanical Engineering at South Dakota State University. He holds a BS in Mechanical Engineering from Nagarjuna University, India. He is interested in mechanical design, strength analysis and computer modeling.

Peer Review: This article has been internationally peer-reviewed and accepted for publication according to the guidelines given at the journal's website.

*Corresponding author (**Z.Hu**). Tel/Fax: +1-605-688-4817. E-mail address: Zhong.Hu@sdstate.edu. American Transactions on Engineering & Applied Sciences. Volume 1 No.2 ISSN 2229-1652 eISSN 2229-1660. Online Available at http://TUENGR.COM/ATEAS/V01/143-161.pdf